# Demonstration of a Dual-Beam Zone Plate for Phase-Contrast Coherent Soft X-ray Imaging

Wei He<sup>a,b</sup>, Antoine Islegen-Wojdyla<sup>a</sup>, Alex Ditter<sup>a</sup>, Rourav Basak<sup>b</sup>, Weilun Chao<sup>c</sup>, Nicolas Burdet<sup>d</sup>, Xiaoya Chong<sup>a</sup>, Chaoying Gu<sup>a</sup>, Alex Frañó<sup>b</sup>, Sujoy Roy<sup>a</sup>, Andreas Scholl<sup>a</sup>, David Shapiro<sup>a</sup>, and Kenneth Goldberg<sup>a</sup>

<sup>a</sup>Advanced Light Source, Lawrence Berkeley National Laboratory, Berkeley, CA 94720, USA.
 <sup>b</sup>Department of Physics, University of California San Diego, La Jolla, CA 92093, USA.
 <sup>c</sup>The Center for X-ray Optics, Lawrence Berkeley National Laboratory, Berkeley, CA 94720, USA.
 <sup>d</sup>Linac Coherent Light Source, SLAC National Accelerator Laboratory, Menlo Park, CA 94025, USA.

#### **ABSTRACT**

Coherent X-ray imaging faces fundamental speed limitations due to computational reconstruction requirements of current phase retrieval methods. We demonstrate dual-beam zone plates that enable direct phase-contrast measurements by structuring coherent X-rays into two focused 110 nm spots separated by 11  $\mu$ m, bypassing iterative algorithms entirely. Experimental validation at the COSMIC beamline confirms precise dual-beam formation with clear interference patterns analogous to Young's double-slit experiment. Comparative measurements reveal enhanced sensitivity: phase detection achieves 45° phase shifts at sample boundaries where intensity contrast exhibits limited signal-to-noise ratio. Spectroscopic demonstrations across the oxygen K-edge show energy-selective capabilities, with phase features providing improved signal-to-noise ratio compared to conventional absorption measurements. The high photon efficiency of this direct measurement approach enables fast imaging capabilities, establishing the technique's suitability for investigating dynamic processes in quantum materials with next-generation synchrotron sources.

**Keywords:** Phase-contrast imaging, Zone plates, Coherent X-ray interferometry, Soft X-rays

#### 1. INTRODUCTION

The advent of 4th generation light sources promises orders of magnitude enhancement in coherent X-ray flux, opening unprecedented opportunities for advanced X-ray imaging.<sup>1,2</sup> These enhanced coherent flux capabilities demand innovative X-ray optical elements that can efficiently utilize the improved beam properties for high-speed measurements.<sup>3</sup> The coherence properties of X-ray radiation have become increasingly central to modern X-ray instrumentation, enabling sophisticated interferometric and diffractive techniques that can probe material structure with exceptional spatial resolution and temporal sensitivity.<sup>4,5</sup>

However, coherent X-ray imaging faces the fundamental "phase problem"—while X-ray interactions modify both amplitude and phase of the electromagnetic field, conventional detectors only measure intensity, losing crucial phase information that encodes structural details.<sup>6,7</sup> Current approaches to phase retrieval rely primarily on iterative computational algorithms such as coherent diffractive imaging and ptychographic reconstruction methods.<sup>8,9</sup> While these techniques have achieved remarkable success, iterative algorithms require extensive processing cycles for convergence, and ptychographic methods demand prolonged data collection with stable experimental conditions. This creates a timing mismatch between the rapid measurement potential enabled by boosted coherent flux and the computational requirements of current phase retrieval approaches.

On the other hand, interferometric X-ray techniques offer compelling alternatives through direct optical encoding of phase information in measurable intensity patterns. For instance, X-ray holography enables imaging applications by creating interference between sample-scattered radiation and a reference beam with two

Further author information: (Send correspondence to W.H.)

W.H.: E-mail: wehe@ucsd.edu A.I.-W.: E-mail: awojdyla@lbl.gov pinholes.<sup>10–12</sup> Similar principles have been demonstrated with double-slit configurations, providing enhanced sensitivity for detecting phase variations in magnetic materials.<sup>13</sup> These interferometric approaches share a common limitation: significant flux loss due to beam-blocking elements that restrict substantial portions of the incident beam.

Dual-beam zone plates (DBZs) represent an innovative approach that combines Fresnel zone plate focusing optics with diffraction grating principles to overcome flux limitations while enabling direct phase-contrast imaging. By structuring incident coherent X-rays into two tightly focused spots with controlled separation, this design enables differential phase measurements while bypassing iterative reconstruction algorithms and preserving beam intensity. This paper presents the first experimental demonstration of DBZ-based phase-contrast measurements at the COSMIC beamline at the Advanced Light Source. We show clear interference fringes analogous to Young's double-slit experiment, enhanced phase sensitivity compared to conventional intensity measurements, and spectroscopic capabilities at atomic absorption edges. The results establish DBZs as a complementary tool for coherent X-ray imaging, particularly suited for applications requiring fast measurements of dynamic processes in quantum materials.

#### 2. METHODS

#### 2.1 Dual-Beam Zone Plate

The DBZ used in this study was fabricated at the Center for X-Ray Optics at Lawrence Berkeley National Laboratory using direct-write electron beam lithography on silicon nitride membranes. The DBZ consolidates the functionalities of a Fresnel zone plate and a grating into a single diffractive optical element through an exclusive-OR (XOR) operation, which overcomes the efficiency limitations of sequential diffractive elements by suppressing the grating's 0th-order diffraction while preserving the zone plate's focusing properties.<sup>14</sup> The XOR pattern can be expressed as:

$$DBZ(x,y) = G(x,y) + ZP(x,y) - 2G(x,y)ZP(x,y)$$
(1)

where G(x, y) represents a binary amplitude grating and ZP(x, y) represents the usual Fresnel zone plate. This design produces multiple diffraction orders, with the two dominant first-order spots providing the primary beams for interferometric measurements.

Figure 1 shows scanning electron microscopy (SEM) images of the fabricated DBZ, which has a total diameter of 240  $\mu$ m with a 95  $\mu$ m central stop, designed for 700 eV photon energy operation with a 12 mm focal length and 0.01 numerical aperture. The integrated grating component with 4.32  $\mu$ m pitch generates two focused spots of approximately 110 nm diameter separated by 10  $\mu$ m at the focal plane.

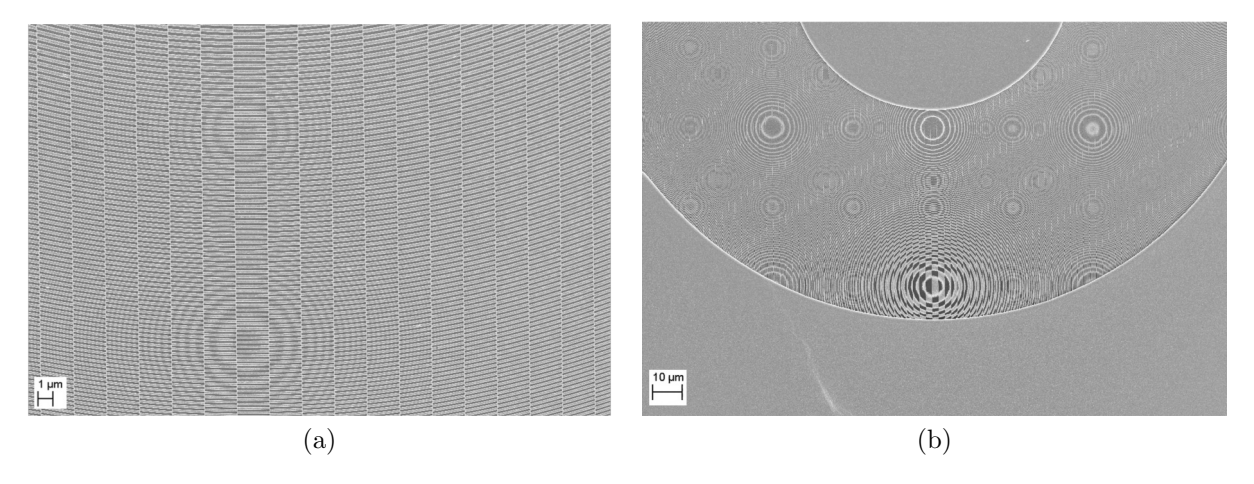


Figure 1. SEM images of the fabricated DBZ. (a) High-magnification view of the zone plate pattern. (b) Overview showing the full DBZ structure with central stop and outer zone regions. Scale bars: (a)  $10 \mu m$ , (b)  $1 \mu m$ .

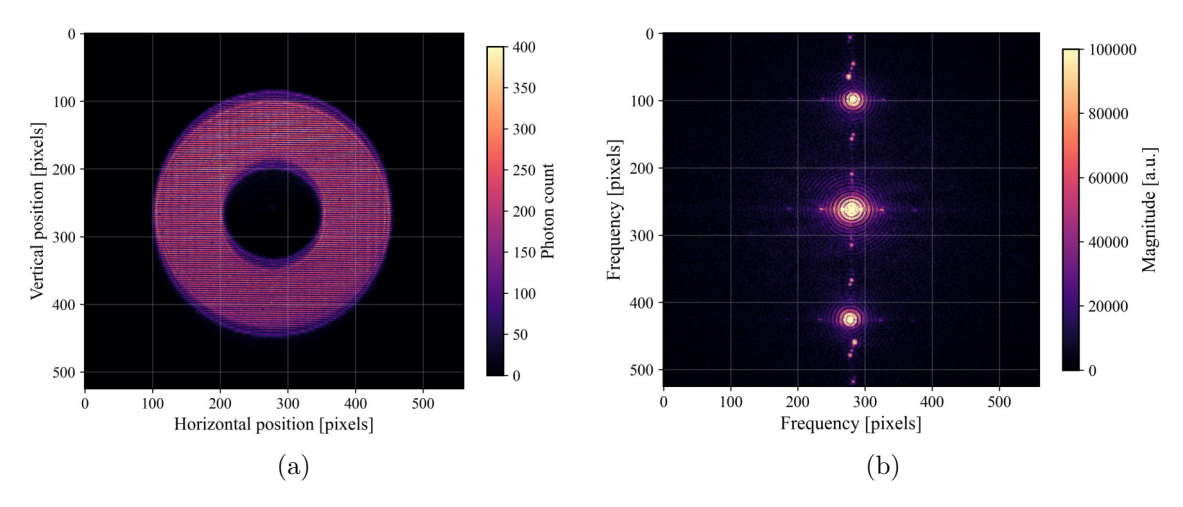


Figure 2. DBZ interference demonstration. (a) Far-field interference pattern recorded with 10 ms exposure time shows circular fringes from coherent beam interference. (b) Two-dimensional FFT reveals the spatial frequency structure: central autocorrelation peak and symmetric side peaks from beam cross-correlations, directly validating the dual-beam architecture. The ring-like structure around each peak reflects finite beam size and coherence properties.

#### 2.2 Experimental Setup and Measurements

The experiment was conducted at the COSMIC beamline (7.0.1.2) at the Advanced Light Source, Lawrence Berkeley National Laboratory. The experimental configuration positioned the DBZ approximately 12 mm upstream of the sample location, with variable distance adjustments to maintain focus at different energies, and a CCD detector (960×960 pixels, 30  $\mu$ m pixel size) located 600 mm downstream to record far-field interference patterns. This scanning transmission X-ray microscopy (STXM) geometry enabled translating the dual-beam position across samples to map spatial variations in both intensity and phase contrasts.

Initial characterization measurements without samples validated the DBZ functionality by recording clear interference fringes analogous to Young's double-slit experiment. Microscopic measurements were performed using nickel-manganese-cobalt oxide samples, where the dual-beam configuration enabled simultaneous measurement of reference and sample regions, with one focused spot positioned on the sample and the other serving as an off-sample reference. Phase-contrast capabilities were demonstrated by translating the dual beams across sample boundaries. Spectroscopic measurements were conducted across the oxygen K-edge to compare phase-contrast detection with conventional absorption spectroscopy.

#### 3. RESULTS AND DISCUSSION

The experimental validation at COSMIC beamline successfully demonstrates the DBZ's ability to structure coherent X-rays into two focused beams. Figure 2a shows the far-field interference pattern recorded at 700 eV photon energy, revealing circular fringes characteristic of coherent beam interference. The circular geometry reflects the radial symmetry of the Fresnel zone plate optic. Analysis of the fringe spacing yields a measured separation of  $\Delta y = 96~\mu m$  on the detector, and using the relationship for far-field interference  $d = \lambda z/\Delta y$  (where  $\lambda$  is the X-ray wavelength of 1.77 nm, z is the propagation distance of 600 mm), we calculate a beam separation of approximately 11  $\mu m$ , which matches exactly with the designed separation. This beam architecture can also be directly visualized by applying a fast Fourier transform (FFT) to the interference pattern (Figure 2b). The analysis reveals three distinct peaks in the spatial frequency domain: an intense central region containing autocorrelations from each beam, and symmetric side peaks arising from cross-correlations that encode the interference information.

Beyond validating the dual-beam architecture, microscopic scanning measurements reveal the enhanced sensitivity of phase-contrast detection over conventional intensity-based methods. The dual beams were translated across sample boundaries in sequential positions, with one beam consistently positioned off-sample as reference

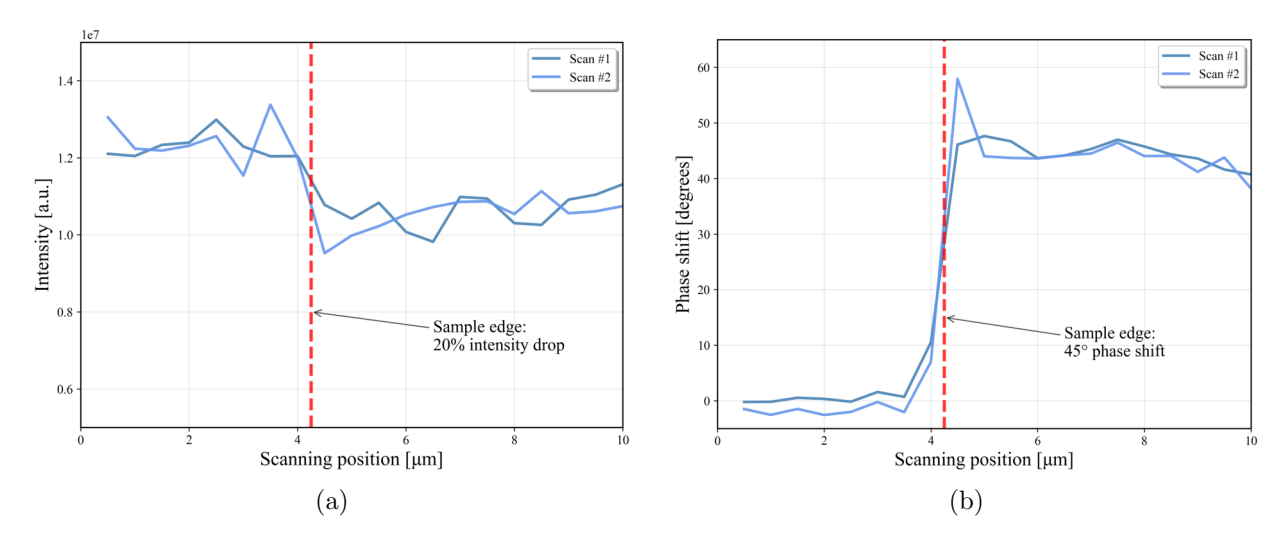


Figure 3. Phase-contrast sensitivity enhancement over intensity-based detection. (a) Intensity measurements exhibit  $\sim 20\%$  transmission changes with poor signal clarity. (b) Phase measurements reveal sharp 45° transitions with excellent reproducibility, demonstrating improved interface detection capabilities. Scan #1 and #2 represent identical measurement types performed at different sample edge locations.

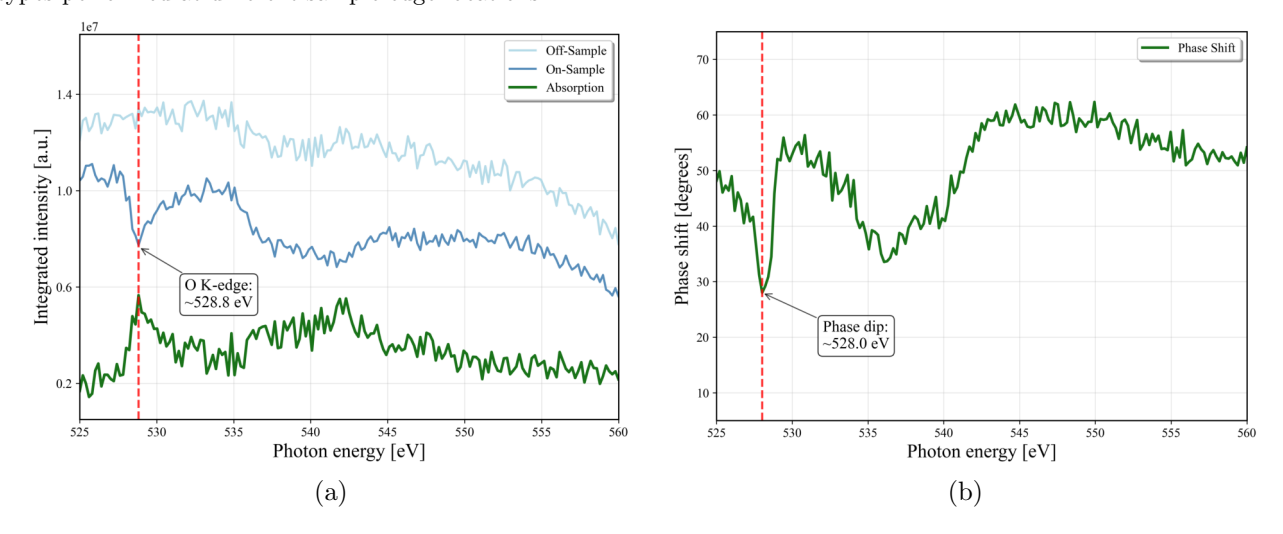


Figure 4. Spectroscopic comparison across the oxygen K-edge region. (a) Conventional absorption spectrum shows characteristic edge structure at  $\sim$ 528.8 eV with significant background fluctuations. (b) Phase shift spectrum reveals enhanced spectral features at  $\sim$ 528.0 eV with better signal-to-noise ratio, demonstrating the energy separation between phase and absorption resonances.

while the other scanned across the sample edge. At each scanning position, transmitted intensity was calculated through pixel integration across the entire ring pattern on the detector, while phase information was extracted through Fourier analysis of the interference fringes, with phase shifts determined from the phase angle of the dominant frequency component following established Fourier transform methods. <sup>14, 15</sup> This comparative analysis demonstrates clear contrast between detection approaches: intensity measurements (Fig. 3a) yielded transmission changes of approximately 20% with noise levels that limited precise interface determination", whereas phase analysis (Fig. 3b) produced improved results with sharp, reproducible transitions and a measured 45° phase shift clearly delineating sample boundaries across independent measurement repetitions. This enhanced contrast sensitivity enables interface detection where intensity variations show minimal change, providing quantitative phase determination through direct interferometric analysis.

Spectroscopic measurements across atomic absorption edges demonstrate element-specific identification capa-

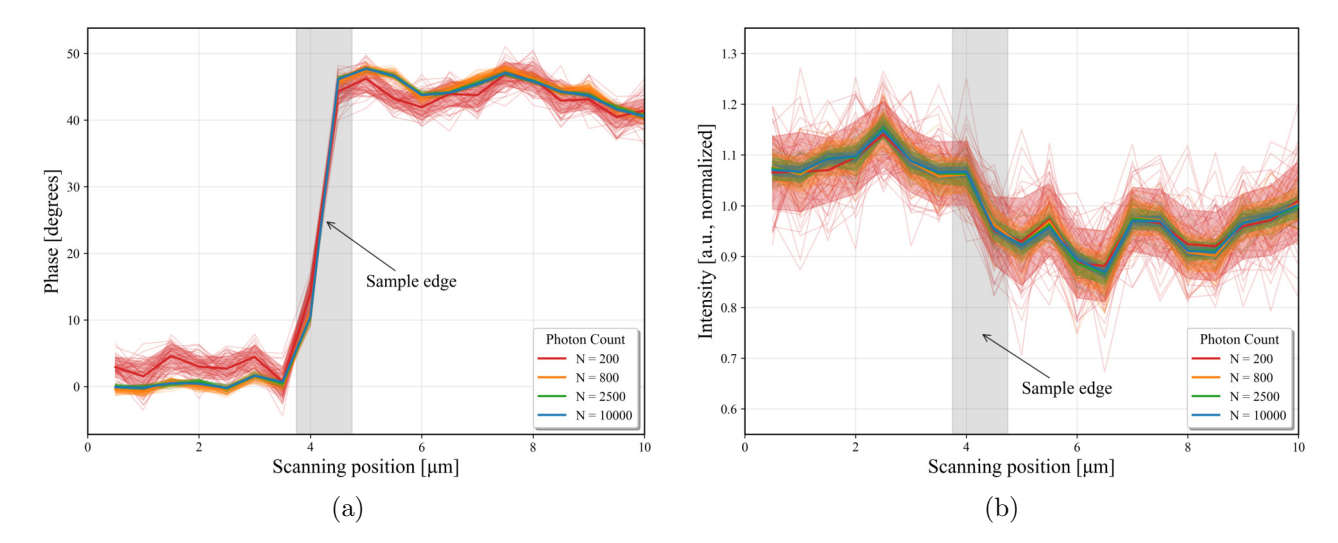


Figure 5. Statistical comparison of detection stability across photon count levels. (a) Phase measurements showing consistent signal clarity with error bands ( $\pm 1\sigma$ , 100 trials) demonstrating minimal noise growth at reduced flux. (b) Intensity measurements exhibiting increased scatter and broader error bands at low photon counts. The 45° phase shift remains detectable across all flux levels, while at N = 200 photons the intensity contrast becomes difficult to distinguish.

bilities through phase-contrast detection. Measurements were performed across the oxygen K-edge region with one beam positioned over sample-free membrane (off-sample reference) while the other interrogated sample-containing regions (on-sample measurement). Conventional absorption spectra were derived by comparing intensity measurements between both-beams-off-sample and one-beam-on-sample configurations, yielding the characteristic edge structure around ~528.8 eV (Fig. 4a). Phase shift measurements were extracted by analyzing the interference pattern changes between these same configurations, revealing spectroscopic features at ~528.0 eV (Fig. 4b). Near absorption resonances, the real (dispersive) and imaginary (absorptive) parts of the complex refractive index exhibit resonant maxima at slightly different energies, <sup>12</sup> with the phase resonance occurring at lower photon energy than the absorption peak. The phase measurements showed improved spectral features with sharper edge structure and reduced background fluctuations compared to conventional absorption measurements, indicating advantages of phase-contrast detection for spectroscopic applications.

The demonstrated performance characteristics establish a foundation for further technical developments that can enhance the DBZ approach. The validated dual-beam formation enables integration with ptychographic reconstruction techniques to characterize detailed spatial profiles of the focused spots, providing independent verification of the dual-beam architecture and beam quality. The successful spectroscopic demonstrations indicate that zone plate designs can be optimized for specific energy ranges and beam separation distances, enabling better matching to different experimental requirements and sample geometries.

The enhanced photon efficiency of phase-contrast detection offers practical advantages for coherent X-ray imaging applications. Figure 5 presents statistical noise analysis comparing phase and intensity detection across different photon count levels using data from Scan #1. To assess detection stability under varying flux conditions, Poisson noise was added to the experimental data to simulate different photon count scenarios, with 100 statistical trials performed for each photon level to evaluate measurement uncertainty. Phase measurements maintain signal-to-noise ratios above 16 at N = 200 photons per measurement, with phase uncertainty below 3°. In contrast, intensity measurements show higher noise sensitivity, with fluctuations increasing significantly at low photon counts. The analysis demonstrates that phase detection achieves reliable measurements with fewer than  $10^3$  photons, while intensity contrast requires higher flux for comparable precision. At the COSMIC beamline's flux of  $\sim 10^9$  photons/s, sub-millisecond exposure times enable measurement rates approaching the MHz regime. This capability makes the technique suitable for studying dynamic processes where iterative reconstruction methods present speed limitations.

These demonstrations establish DBZ performance characteristics that provide complementary capabilities

to existing coherent X-ray imaging methods. The high phase sensitivity enables measurements of index of refraction changes in ultra-thin materials where conventional absorption contrast provides insufficient signal. The fast measurement capability suits investigations of rapid domain dynamics and phase transitions in quantum materials where temporal resolution has been challenging to achieve. Future work can explore these applications as next-generation synchrotron sources provide enhanced coherent flux.

#### 4. SUMMARY

This work presents the first successful demonstration of dual-beam zone plates for direct phase-contrast X-ray imaging, establishing an approach that bypasses computational reconstruction requirements of conventional coherent imaging methods. Experimental validation at the COSMIC beamline confirms precise dual-beam formation with 11  $\mu$ m separation, producing clear interference patterns that enable quantitative phase measurements through direct Fourier analysis. Comparative microscopy measurements reveal enhanced sensitivity, with phase detection achieving 45° phase shifts at sample boundaries where intensity contrast shows 20% transmission changes accompanied by significant noise. Spectroscopic demonstrations across the oxygen K-edge show energy-selective capabilities, with phase features at 528.0 eV providing improved signal-to-noise ratio compared to conventional absorption measurements at 528.8 eV.

The technique's photon efficiency—requiring fewer than 10<sup>3</sup> photons for reliable phase contrast—enables measurement rates approaching the MHz regime at typical synchrotron flux levels, positioning DBZ-based imaging to exploit enhanced coherent flux from next-generation synchrotron sources for investigating dynamic processes in quantum materials.

### ACKNOWLEDGMENTS

This work is supported by an Early Career Award in the X-Ray Instrumentation Program funded by the Department of Energy Office of Basic Energy Sciences (BES), Contract No. DE-AC02-05CH11231. W.H. was supported in part by an ALS Collaborative Postdoctoral Fellowship.

## REFERENCES

- [1] White, A., Goldberg, K., Kevan, S., Leitner, D., Robin, D., Steier, C., and Yarris, L., "A new light for berkeley lab—the advanced light source upgrade," *Synchrotron Radiation News* **32**(1), 32–36 (2019).
- [2] Khubbutdinov, R., Menushenkov, A. P., and Vartanyants, I. A., "Coherence properties of the high-energy fourth-generation X-ray synchrotron sources," *Journal of Synchrotron Radiation* **26**(6), 1851–1862 (2019).
- [3] Eriksson, M., van der Veen, J. F., and Quitmann, C., "Diffraction-limited storage rings a window to the science of tomorrow," *Journal of Synchrotron Radiation* **21**(5), 837–842 (2014).
- [4] Li, P., Allain, M., Grünewald, T. A., Rommel, M., Campos, A., and Carbone, D., "4th generation synchrotron source boosts crystalline imaging at the nanoscale," *Light: Science & Applications* 11, 73 (2022).
- [5] Dietze, S. H. and Shpyrko, O. G., "Coherent diffractive imaging: towards achieving atomic resolution," Journal of Synchrotron Radiation 22(6), 1498–1508 (2015).
- [6] Miao, J., Ishikawa, T., Robinson, I. K., and Murnane, M. M., "Beyond crystallography: Diffractive imaging using coherent x-ray light sources," *Science* **348**(6234), 530–535 (2015).
- [7] Chapman, H. N. and Nugent, K. A., "Coherent lensless x-ray imaging," Nature Photonics 4(12), 833–839 (2010).
- [8] Pfeiffer, F., "X-ray ptychography," Nature Photonics 12(1), 9–17 (2018).
- [9] Thibault, P., Dierolf, M., Menzel, A., Bunk, O., David, C., and Pfeiffer, F., "High-resolution scanning x-ray diffraction microscopy," *Science* **321**(5887), 379–382 (2008).
- [10] Eisebitt, S., Lüning, J., Schlotter, W. F., Lörgen, M., Hellwig, O., Eberhardt, W., and Stöhr, J., "Lensless imaging of magnetic nanostructures by x-ray spectro-holography," Nature 432(7019), 885–888 (2004).
- [11] Fuhse, C., Ollinger, C., and Salditt, T., "Waveguide-based off-axis holography with hard x rays," *Phys. Rev. Lett.* **97**, 254801 (2006).

- [12] Scherz, A., Schlotter, W. F., Chen, K., Rick, R., Stöhr, J., Lüning, J., McNulty, I., Günther, C., Radu, F., Eberhardt, W., Hellwig, O., and Eisebitt, S., "Phase imaging of magnetic nanostructures using resonant soft x-ray holography," *Phys. Rev. B* **76**, 214410 (2007).
- [13] Atkar, S., Tumbleson, Z., Morley, S. A., Burdet, N., Islegen-Wojdyla, A., Goldberg, K. A., Scholl, A., Montoya, S. A., Datta, T., and Roy, S., "Magnetically modified double slit based x-ray interferometry," (2025).
- [14] Chang, C., Anderson, E., Naulleau, P., Gullikson, E., Goldberg, K., and Attwood, D., "Direct measurement of index of refraction in the extreme-ultraviolet wavelength region with a novel interferometer," *Optics Letters* 27(12), 1028–1030 (2002).
- [15] Goldberg, K. A. and Bokor, J., "Fourier-transform method of phase-shift determination," Appl. Opt. 40(17), 2886–2894 (2001).